

A GENERAL FRAMEWORK FOR SUPPORTING ECONOMIC FEASIBILITY OF GENERATOR AND STORAGE ENERGY SYSTEMS THROUGH CAPACITY AND DISPATCH OPTIMIZATION

Saeed Azad*

Postdoctoral Fellow

Department of Systems Engineering
Colorado State University
Fort Collins, CO 80523

saeed.azad@colostate.edu

Ziraddin Gulumjanli

Graduate Student

Department of Systems Engineering
Colorado State University
Fort Collins, CO 80523

ziraddin.gulumjanli@colostate.edu

Daniel R. Herber

Assistant Professor

Department of Systems Engineering
Colorado State University
Fort Collins, CO 80523

daniel.herber@colostate.edu

ABSTRACT

Integration of various electricity generating technologies (such as natural gas, wind, nuclear, etc.) with storage systems (such as thermal, battery electric, hydrogen, etc.) has the potential to improve the economic competitiveness of modern energy systems. Driven by the need to efficiently assess the economic feasibility of various energy system configurations in early system concept development, this work outlines a versatile computational framework for assessing the net present value of various integrated storage technologies. The subsystems' fundamental dynamics are defined, with a particular emphasis on balancing critical physical and economic domains to enable optimal decision-making in the context of capacity and dispatch optimization. In its presented form, the framework formulates a linear, convex optimization problem that can be efficiently solved using a direct transcription approach in the open-source software DTQP. Three case studies are considered to demonstrate and validate the capabilities of the framework, highlighting its value and computational efficiency in facilitating economic assessment of various configurations of energy systems. In particular, natural gas with thermal storage and carbon capture, wind energy with battery storage, and nuclear with hydrogen are demonstrated.

Keywords: control co-design, integrated energy systems, generator & storage, capacity & dispatch, techno-economic analysis

1 INTRODUCTION

The ever-changing and increasing energy demand resulting from various technological advancements, such as renewable energy

and vehicle electrification, has significantly affected various aspects of the energy market, from energy supply networks to transportation, storage, and consumption. This increase in electricity demand coincides with environmental policies that dictate more stringent requirements on carbon emissions. Furthermore, the stability of the electrical grid and the profitability of energy producers will depend on more reliable and flexible production. To adapt to such policies while meeting the increasing energy demands of our society, a promising solution is the integration of various generation and storage systems [1]. This solution offers an integrated approach towards energy systems and is positioned to revolutionize the energy market economy [2].

This approach, which is closely related to *integrated energy systems* (IES) [1] and *hybrid energy systems* (HES) [3] offers an increase in flexibility and robustness of the energy supply/demand [4]. It also promotes new business models for some utility companies to better adapt to scientific, technological, political, and socio-economic developments. Since many utility companies are commercial units, their sustainable operation hinges on consistent generation of revenue. However, the combination of higher penetration of renewable energy sources, volatile fossil fuel prices, more stringent environmental policies, etc. can negatively affect the economic competitiveness of some technologies.

For example, the most expensive per unit electricity, which is typically produced by nuclear power (due to complexity, capital intensiveness, construction time, etc.), is purchased last during peak demand when other sources are not available. This, along with other factors such as costs of repair, has resulted in the retirement of over 12 nuclear power plants (NPP) from February 2013 through April 2021 [5]. The retirement of NPPs, which roughly produce a fifth of the total electricity generation and half

*Corresponding author, saeed.azad@colostate.edu

of the non-fossil fuel-based electricity in the U.S. (with no intermittency), points to a changing energy landscape in which NPPs require flexibility in base load to remain competitive [6].

A potential solution is to increase the economic competitiveness of such technologies by configuring them as a part of integrated energy systems, operating simultaneously with other generators, functions such as carbon capture and storage (CCS), and energy storage units. In the case of the NPP, for example, the plant may supply power to the grid when the electricity prices are high and store energy during periods of oversupply. Depending on the storage type, the stored energy can then be directly sold as electricity or in the form of another energy/commodity, such as thermal energy or hydrogen. The thermal energy can be directly sold to chemical plants for use in industrial processes, while hydrogen can be either combusted to generate additional electricity [7] or sold for use in fuel cells, or steel manufacturing industry.

To be economically beneficial, the flexibility added by incorporating these generators in the context of integrated energy systems must be sufficient to overcome the capital and operational cost of the technology over its lifetime. A techno-economic assessment, presented here as a net present value (NPV) objective, is often at the core of analyzing how the integration of new units (such as generator and storage), functions (such as CCS, district heating/cooling, etc), can affect the economy of the entire system. It is also central to any retrofit design efforts within a structured energy system.

To maximize NPV, optimization of storage capacities (i.e., plant variables), along with the optimization of requested power, charge, and discharge decisions (i.e., control variables) must be performed within the context of capacity and dispatch optimization. This combination and consideration of design decisions is referred to as control co-design (CCD) [8]. This class of problems has been explored in the context of integrated energy systems for natural gas combined cycle (NGCC) with thermal energy storage (TES) and CCS [9], light water reactor (LWR) with various TES technologies [6], and nuclear power plant with hydrogen production [10].

The resulting dynamic optimization problem, when used with high-fidelity, non-linear technical models, is often computationally expensive. For example, to reduce the computational cost, instead of solving the problem for an entire year, Ref. [11] considered a 24-hour horizon, and solved the problem 365 times. For effective early-stage decision-making, ideally, only a few assumptions and adjustments need to be added beyond the core techno-economic ones needed for assessment. Therefore, there is a need for an efficient and versatile computational framework that can capture subsystems' basic dynamics, constraints, and NPV economic analysis to assess various system configurations and scenarios for integrated generator and storage energy systems.

This computational framework is further motivated by the fact that feasibility studies of various system configurations/ar-

chitectures are often required before selecting the most profitable option. Accounting for subsystems' basic dynamics offers flexibility in assessing different system architectures without spending an unreasonable amount of resources on the development, construction, and optimization of high-fidelity models. Given that specific system components, characteristics, and performance criteria are often unknown in early-stage design and will be determined in later steps, the balance of fidelity maintained in the proposed framework enables the evaluation of overall system performance without the need for the determination of specific subsystems and components. Finally, a versatile framework should assist in navigating the decision-making process among engineers with technical expertise in the field and those with limited backgrounds, such as stakeholders and investors, who are often among the primary decision-makers in the space.

Therefore, this article presents the development and demonstration of an open-source framework in MATLAB for assessing the *economic feasibility of generator and storage systems through CCD*, which we refer to as ECOGEN-CCD. Empowered by subsystems' basic dynamics, ECOGEN-CCD formulates the capacity & dispatch dynamic optimization problem that can be efficiently implemented and solved using the open-source MATLAB software DTQP [12, 13], which uses direct transcription with an automatic problem generation for linear-quadratic dynamic optimization problems. This improvement in efficiency is highlighted by the fact that ECOGEN-CCD, in its current form, is capable of solving a capacity and dispatch dynamic optimization problem with an hourly mesh for 30 years in less than 300 [s]. Compared with the tools utilized in Refs. [14] and [5], ECOGEN-CCD emphasizes the design and operation of an individual plant, consisting of a collection of generators, storage units, and functions. ECOGEN-CCD is an open-source tool that is made publicly available in Ref. [15].

The remainder of the article is organized in the following manner: Sec. 2 starts by describing some motivations for the proposed framework and then discusses framework architecture, problem elements, techno-economic considerations, and problem formulation; Sec. 3 is focused on the demonstration of the proposed framework using three case studies with different generator and storage technologies including an NGCC with TES and CCS, wind energy with battery energy storage, and an NPP with hydrogen generation and storage; and Sec. 4 offers some remarks regarding conclusions, limitations, and future directions of the study.

2 PROBLEM DESCRIPTION

In this section, we describe the IES architecture, problem elements, techno-economic considerations, and the capacity and dispatch optimization problem.

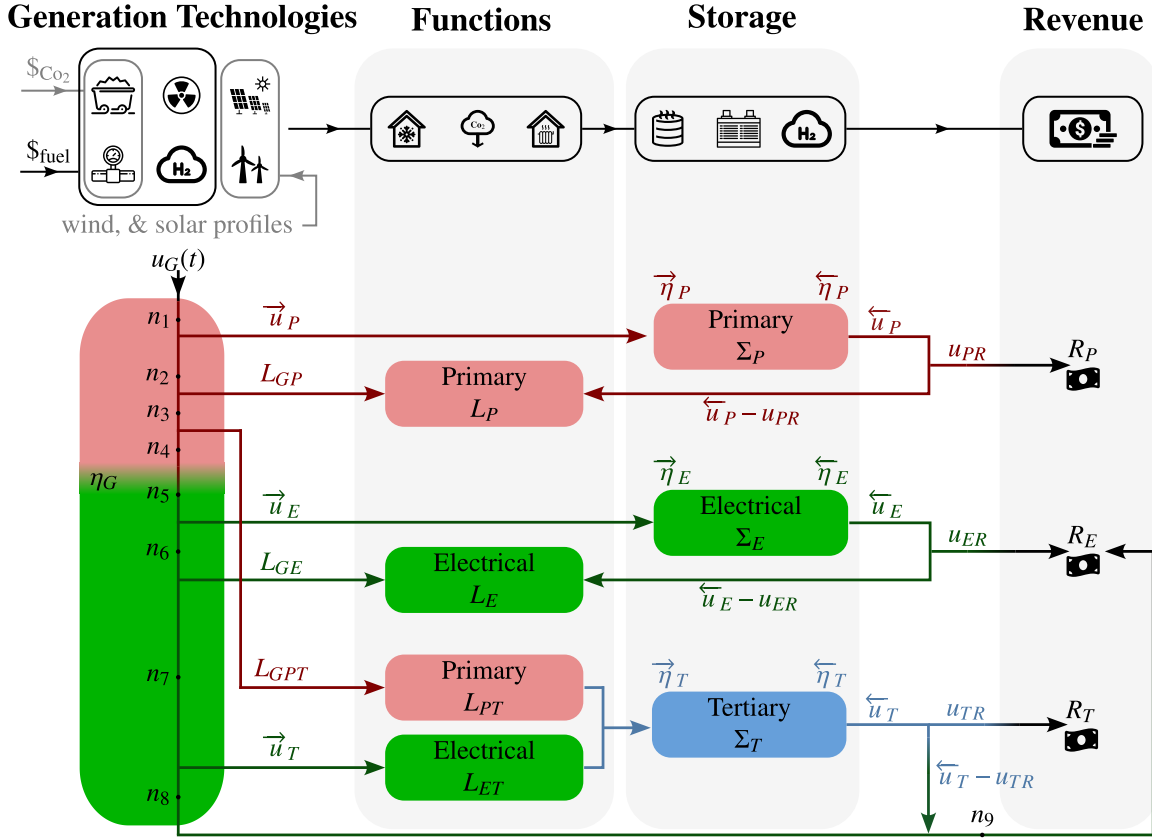


FIGURE 1: Illustration of an IES architecture with a collection of homogeneous electric power generators, and three types of storage systems. Primary (such as thermal), electrical (such as battery), and tertiary (such as hydrogen) storage is shown in red, green, and blue, respectively. The charge and discharge signals, along with their associated efficiencies, are described by $\vec{\eta}$, and $\overleftarrow{\eta}$, respectively.

2.1 IES Architecture

Figure 1 describes the general architecture of an integrated energy system (IES) considered in this framework. An IES is characterized by various generators (e.g., NGCC power plant, wind farm, or NPP) and storage unit (e.g., TES, battery energy storage system (BESS), or hydrogen storage). Additional functions (e.g., CCS, district heating/cooling, etc.) may also be present in the system and are characterized by the addition of their associated costs and energy requirements.

The generator, which is described by the subscript \bullet_G , is the unit responsible for producing electricity from an energy vector (e.g., natural gas) by often converting it first to a primary energy domain (e.g., thermal energy), and ultimately converting it to electricity with efficiency of η_G :

$$\text{generator's primary energy domain} \xrightarrow{\eta_G} \text{electricity} \quad (1)$$

Based on the desired configuration, the generator may have access to three different types of storage systems, distinguished through the subscript \bullet_S . These storage systems are defined based on their key energy domain. The first storage system uses

the generator's primary domain, \bullet_P , to store energy. As an example, in an NGCC power plant, the primary energy domain is thermal energy. Thus, the primary storage system for this generator is a TES unit. In this work, the secondary energy domain is always electrical, \bullet_E . Therefore, the second storage type directly stores energy as electricity (e.g., through a BESS). A third storage facility, \bullet_T , is included to enable the usage of electricity to create a new product, commodity, service, or energy storage in a distinct medium, such as hydrogen.

The storage system is characterized by charge $\vec{\eta}$ and discharge $\overleftarrow{\eta}$ signals (noting the arrow directions). The charge signal can be affected by losses during the transmission. Therefore, its efficiency is denoted by $\vec{\eta}_*$. The output efficiency of the storage is described as $\overleftarrow{\eta}_*$:

$$\text{charging signal} \xrightarrow{\vec{\eta}_*} \text{storage} \quad (2a)$$

$$\text{storage} \xrightarrow{\overleftarrow{\eta}_*} \text{discharge signal} \quad (2b)$$

This systematic separation of efficiencies allows us, in the future, to consider additional factors, such as the distance be-

tween the facilities, which can affect the efficiency of energy transmission. An additional revenue-driven control signal, represented by \bullet_R , is responsible for deciding the percentage of the discharge signal that is immediately turned into revenue through direct sales. For example, the revenue signal will decide how much of the discharged hydrogen is sold at current hydrogen prices. The remaining product will be combusted and sold as electricity.

The inclusion of various functions may result in the presence of additional load requirements. For example, in addition to auxiliary electrical loads, the operation of a CCS unit, which is assumed to be in operation whenever the generator is on, requires additional thermal and electrical loads. These loads are a function of the current power level of the generator, presented as a certain percentage of the power plant power level. Similarly, a high-temperature steam electrolysis (HTSE) process in a hydrogen plant (tertiary storage) requires both thermal and electrical energy, however, these load requirements are active only when a decision is made to generate hydrogen from the excess electricity. Therefore, these loads are a function of the tertiary charging signal, presented as a certain percentage of its current value.

The top part of Fig. 1 highlights some considerations regarding the electric energy technologies, including fuel cost, carbon tax, and dispatchable versus non-dispatchable type of resources. The bottom part presents a case for a collection of homogeneous generators (e.g., a wind farm) in the presence of multiple functions and storage types. The nodes in this figure, which are described by n_1, \dots, n_9 are used to formulate some of the necessary constraints within the optimization problem and are mathematically described in Appendix A.

2.2 Problem Elements

This section introduces some problem elements based on the comprehensive case in which a collection of homogeneous generators have potential access to all 3 storage types in the presence of both primary and electrical loads. Adding the capability of simultaneously working with multiple non-homogeneous generators will be a future step of this work. Similarly, in the future, we plan to enable a more advanced integration of storage units in the toolbox, such that multiple storage topologies (e.g., two battery storage and one hydrogen storage) can be simultaneously integrated with ECOGEN-CCD.

Plant Variables: The capacity of each storage type is a sizing decision that will be determined by the optimizer, and constitutes the plant optimization variables Σ :

$$\Sigma = [\Sigma_P, \Sigma_E, \Sigma_T]^T \quad (3)$$

Note that the vector of plant optimization variables reduces in size if the study does not include all three storage types.

Control Variables: Every energy storage system entails 3 control variables, one for charging the storage (\vec{u}_*), one for dis-

charging the storage \vec{u}_* , and one for determining the fraction of discharge u_{*R} that is directly used to generate revenue without any intermediate steps. In addition, the operator can request a specific power from the generator through a control command, described as $u_G(t)$. The vector of control variables can then be defined as:

$$\begin{aligned} \mathbf{u}(t) &= [u_G(t), \mathbf{u}_S(t)]^T \\ &= [u_G(t), \mathbf{u}_{SP}(t), \mathbf{u}_{SE}(t), \mathbf{u}_{ST}(t)]^T \end{aligned} \quad (4)$$

Here, every storage control vector $\mathbf{u}_{S*}(t)$ consists of 3 variables $\mathbf{u}_{S*}(t) = [\vec{u}_*(t), \vec{u}_*(t), u_{*R}(t)]^T$. Similar to the previous case, the size of the control vector will be reduced if only some of the storage types are included in the study.

State Variables: There is one state variable associated with the generator which describes the power level of the generator using a ramp rate of τ :

$$\dot{x}_G(t) = \frac{1}{\tau}(-x_G(t) + u_G(t)) \quad (5)$$

Each storage system is characterized by a state variable that describes the current amount of stored energy in that system. For the most comprehensive case with 3 different storage facilities, the storage dynamics are described by:

$$\dot{\mathbf{x}}_S(t) = \begin{bmatrix} \dot{x}_P(t) \\ \dot{x}_E(t) \\ \dot{x}_T(t) \end{bmatrix} = \begin{bmatrix} \overbrace{\vec{\eta}_P \vec{u}_P(t)}^{\text{Charge}} \\ \overbrace{\vec{\eta}_E \vec{u}_E(t)}^{\text{Discharge}} \\ \overbrace{\alpha_{ET} \vec{\eta}_T \vec{u}_T(t)}^{\text{Discharge}} \end{bmatrix} - \begin{bmatrix} \overbrace{\vec{u}_P(t)}^{\text{Discharge}} \\ \overbrace{\vec{u}_E(t)}^{\text{Discharge}} \\ \overbrace{\vec{u}_T(t)}^{\text{Discharge}} \end{bmatrix} \quad (6)$$

where α_{ET} is the conversion rate between electricity and the tertiary commodity. Describing storage states in vector form and augmenting them with generator state, the dynamics of the problem is described by:

$$\begin{aligned} \dot{\mathbf{x}}(t) &= \mathbf{A}\mathbf{x}(t) + \mathbf{B}\mathbf{u}(t) \\ \begin{bmatrix} \dot{x}_G(t) \\ \dot{\mathbf{x}}_S(t) \end{bmatrix} &= \begin{bmatrix} -1/\tau & \mathbf{0} \\ \mathbf{0} & \mathbf{0} \end{bmatrix} \begin{bmatrix} x_G(t) \\ \mathbf{x}_S(t) \end{bmatrix} + \begin{bmatrix} 1/\tau & \mathbf{0} \\ \mathbf{0} & \mathbf{b}_S \end{bmatrix} \begin{bmatrix} u_G(t) \\ \mathbf{u}_S(t) \end{bmatrix} \end{aligned} \quad (7)$$

where \mathbf{b}_S is the appropriately-sized matrix:

$$\mathbf{b}_S = \begin{bmatrix} \vec{\eta}_P & -1 & 0 & 0 & 0 & 0 & 0 & 0 & 0 \\ 0 & 0 & 0 & \vec{\eta}_E & -1 & 0 & 0 & 0 & 0 \\ 0 & 0 & 0 & 0 & 0 & 0 & \alpha_{ET} \vec{\eta}_T & -1 & 0 \end{bmatrix} \quad (8)$$

Constraints: This section presents all of the time-independent and time-dependent constraints in the dynamic optimization problem.

The storage capacities are non-negative. Therefore, the following constraint is imposed on plant variables:

$$\mathbf{0} \leq \Sigma \quad (9)$$

The requested power from the generator is non-negative and less or equal to the net nominal capacity of the generator. Similarly, the charge and discharge signals are non-negative and never greater than the maximum energy transfer rate into and out of

the storage system, respectively. These maximum and minimum energy transfer rates are currently input parameters, but will be added to the set of potential plant optimization variables in the future, similar to Ref. [9]. These constraints are succinctly described in vector form as:

$$\mathbf{0} \leq \mathbf{u}(t) \leq \mathbf{u}_{\max} \quad (10a)$$

Specifically, the revenue-generating fraction of the control signal in Eq. (10) is non-negative and equal to or smaller than the discharge signal:

$$u_{PR}(t) \leq \overleftarrow{u}_P(t) \quad (10b)$$

$$u_{ER}(t) \leq \overleftarrow{u}_E(t) \quad (10c)$$

$$u_{TR}(t) \leq \overleftarrow{u}_T(t) \quad (10d)$$

Generator's power level must remain non-negative and never exceed its nominal capacity. Requesting a specific (admissible) power output from the generator is reasonable for technologies such as nuclear or NGCC under simplifying assumptions like no temperature-dependence on its operation or maintenance schedules. For intermittent technologies, such as wind and solar, they are at the mercy of the availability of (renewable) resources. In other words, the electricity produced by such technologies is not dispatchable due to the inherent intermittency of the resource. Thus, it is necessary to ensure that the generator state $x_G(t)$ is bounded by an input signal that represents the level of resource availability. These result in the following constraint on generator's state:

$$\mathbf{0} \leq \mathbf{x}_G(t) \leq \mathbf{x}_{G,\max}(t) \quad (11)$$

where $\mathbf{x}_G(t)$ refers to the generator's state, and $\mathbf{x}_{G,\max}(t)$ is an upper bound that is established based on nominal capacity, or the availability of renewable resources. Further details regarding the construction of $\mathbf{x}_{G,\max}(t)$ for a wind farm are included in Sec. 3.2.

The amount of stored energy must be non-negative and less or equal to the capacity of the storage system:

$$\mathbf{0} \leq \mathbf{x}_S(t) \leq \mathbf{\Sigma} \quad (12)$$

which represents a key coupling between select states and the plant parameters.

The initial states are prescribed for all the state variables. It is also assumed that at the final time t_f , the storage system has the same amount of stored energy at t_0 :

$$\mathbf{x}(t_0) = \mathbf{x}_0 \quad (13a)$$

$$\mathbf{x}_S(t_f) = \mathbf{x}_S(t_0) \quad (13b)$$

where the latter equation is optional as multiple shorter, sequential time horizons do not necessitate this assumption [9].

In addition to the upper bound imposed by the maximum energy transfer rate for charging the storage system (Eq. 10), it is necessary to ensure that the charging signal is smaller or equal to the available power in the generator. This is described with the

help of nodes that are placed in Fig. 1:

$$\overrightarrow{u}_P(t) \leq n_1(t) \quad (14a)$$

$$\overrightarrow{u}_E(t) \leq n_5(t) \quad (14b)$$

$$\overrightarrow{u}_T(t) \leq n_7(t) \quad (14c)$$

where the mathematical expressions associated with all of the nodes n_1, \dots, n_9 are provided in Appendix A.

In addition, the generator's load-satisfying signals L_{GP} , L_{GE} , and L_{PT} are non-negative. This condition is to ensure that power does not flow from the storage system into the generator. These signals are also upper-bounded by the available power in the generator. These constraints are formulated as:

$$\mathbf{0} \leq L_{GP}(t) \leq n_2(t) \quad (15a)$$

$$\mathbf{0} \leq L_{GPT}(t) \leq n_3(t) \quad (15b)$$

$$\mathbf{0} \leq L_{GE}(t) \leq n_5(t) \quad (15c)$$

Objective Function: The net present value (NPV) objective function, which enables the assessment of the economic viability of a given technology, is used in this framework. NPV is calculated as:

$$\text{maximize NPV} = -C_{\text{cap}}(\mathbf{\Sigma}) + \int_{t_0}^{t_f} \frac{v_{\text{profit}}(\mathbf{u}, \mathbf{x}, \mathbf{\Sigma}, t)}{D(t)} dt \quad (16)$$

where C_{cap} are the capital expenses, $v_{\text{profit}}(t)$ is calculated as a function of expenses and revenues, and $D(t)$ is the discounting function (money is 'worth' more now than in the future). An annualized discounting function is considered here as:

$$D(t) = (1 + r)^{\text{year}(t)} \quad (17)$$

where r is the discount rate and $\text{year}(t)$ is the integer number of years that have passed since t_0 . These intermediate quantities are now discussed in detail.

2.3 Techno-Economic Considerations

In order to construct the NPV objective function in Eq. (16), we first consider the sources of costs and revenues. These cost parameters are a user-defined input to the ECOGEN-CCD framework.

2.3.1 Expenses All of the costs included in techno-economic analysis, including capital costs, fixed and variable operation and maintenance, fuel costs, and carbon cost are described in this section.

Capital Costs: In this article, we assume that the capital cost, C_{cap} consists of overnight capital costs C_{occ} , and costs over the period of construction C_{cp} :

$$C_{\text{cap}} = C_{\text{occ}} + C_{cp} \quad (18)$$

where C_{occ} assumes that all of the construction occurs overnight. Therefore, this term exclude changes in the prices of goods and financial costs (such as loan, inflation, discount rate, etc.). This allows potential investigations into the impact of construction pe-

riods, rates of inflation, etc. in the analysis [16]. C_{occ} consists of direct construction costs, indirect construction costs, contingencies, and owner's cost, explained in detail in Ref. [17, 18].

C_{cp} includes all the costs that are incurred over the construction period, such as escalation, loan, inflation, etc. Therefore, this term is sensitive to the choice of financial parameters such as discount rate, debt-equity ratio, interest rate, interest during construction (IDC), etc. In this study, we simplify this term, similar to the methodology presented in Ref. [19], to account for the costs over the period of construction through a simple model characterizing IDC:

$$C_{cap} = C_{occ}(1 + C_{idc}) \quad (19)$$

where C_{idc} is calculated as a function of the construction time T_{con} , and the cost of capital rate r , estimated as:

$$C_{idc} = \frac{r}{2}T_{con} + \frac{r^2}{6}T_{con}^2 \quad (20)$$

Inclusion of more advanced financial parameters [9], such as loan, depreciation, etc. are future work items for this framework. For the entire system, the capital cost is expressed as:

$$C_{cap} = [C_{occ_G} + C_{occ_P}\Sigma_P + C_{occ_E}\Sigma_E + C_{occ_T}\Sigma_T](1 + C_{idc}) \quad (21)$$

Operation and Maintenance (O&M): The main elements included in O&M costs are associated with fixed and variable O&M costs. Fixed O&M costs, expressed as C_{fom} , include regular system maintenance, decommissioning, component replacement, etc. These costs only depend on the duration of the operation. For storage systems, these costs scale with storage size (e.g., more frequent and lengthier maintenance for larger capacities). Fixed O&M costs C_{fom} are then calculated as:

$$C_{fom}(t) = C_{fom_G} + C_{fom_P}\Sigma_P + C_{fom_E}\Sigma_E + C_{fom_T}\Sigma_T \quad (22)$$

Variable O&M costs, expressed as C_{vom} , reflect the non-fuel portion of the costs that vary by the amount of energy generated or supplied (such as water, waste disposal, lubricants, chemicals, and other consumable materials). Therefore, these costs depend on the power level of the unit, expressed as:

$$C_{vom}(t) = C_{vom_G} + C_{vom_P}(\vec{\eta}_P \vec{u}_P(t) + \vec{u}_P(t)) \quad (23a)$$

$$+ C_{vom_E}(\vec{\eta}_E \vec{u}_E(t) + \vec{u}_E(t)) \quad (23b)$$

$$+ C_{vom_T}(\alpha_{ET}\vec{\eta}_T \vec{u}_T(t) + \vec{u}_T(t)) \quad (23c)$$

Fuel Costs: Generally, fuel cycle cost, $C_{fuel}(t)$ includes both front-end and back-end costs, such as supply, conversion, enrichment, fabrication, transportation, and waste disposal. For fossil fuels, the cost of fuel only entails the front-end costs, as received from the market. However, for nuclear power plants, the back-end costs are also included as a percentage of the front-end costs:

$$E_{fuel}(t) = \rho_{fuel}C_{fuel}(t)x_G(t) + B_{fuel}(t) \quad (24)$$

where ρ_{fuel} is the conversion factor between the power output of the generator and fuel consumed, $C_{fuel}(t)$ is the instantaneous fuel prices, and $B_{fuel}(t)$ is the back-end cost (again, mainly necessary

for waste management and disposal in nuclear power plants).

Carbon Cost: With the goal of making the societal cost of carbon emissions visible, carbon cost, expressed as C_{Co_2} , assumes a carbon tax rate to incentivize clean electricity generation. The cost of fuel, is therefore estimated as:

$$E_{Co_2}(t) = C_{Co_2}\alpha_{Co_2}\rho_{fuel}x_G(t) \quad (25)$$

where C_{Co_2} is the carbon tax, and α_{Co_2} is the amount of Co_2 produced per unit of fuel.

2.3.2 Revenue: Here, the operator can earn revenue by either directly selling electricity to the grid (without using storage), or alternatively, using storage to sell primary energy, electricity, or a tertiary commodity. The total revenue is calculated for all energy domains as a function of their associated prices. The price arbitrage between primary, electricity, and tertiary domains determines the optimal flow of energy that maximizes the objective function. As an example, revenue earned by selling stored thermal energy to chemical plants (first term in Eq. (26)) is calculated as a function of thermal energy prices $C_P(t)$, discharge efficiency $\vec{\eta}_P$, and the revenue control signal $u_{PR}(t)$. The revenue control signal, however, may only become active when the electricity prices are low and thermal energy prices are high. Note that for certain commodity types, such as hydrogen, it is also possible to generate electricity which will then be sold to the grid. Mathematically, the revenue can be described as:

$$\begin{aligned} R = & R_P(t) + R_E(t) + R_T(t) \\ = & C_P(t)\vec{\eta}_P u_{PR}(t) + C_E(t)\eta_G x_G(t) - C_E(t)\eta_G \vec{u}_P(t) \\ & - C_E(t)\eta_G L_P x_G(t) + C_E(t)\eta_G \vec{\eta}_P \vec{u}_P(t) \\ & - C_E(t)\eta_G \vec{\eta}_P u_{PR}(t) - C_E(t)\eta_G L_{PT} \vec{u}_T - C_E(t)\vec{u}_E(t) \\ & - C_E(t)L_E x_G(t) + C_E(t)\vec{\eta}_E \vec{u}_E(t) - C_E(t)\vec{u}_T(t) \\ & + \alpha_{TE}C_E(t)\vec{\eta}_T \vec{u}_T(t) - \alpha_{TE}C_E(t)\vec{\eta}_T u_{TR}(t) \\ & + C_T(t)\vec{\eta}_T u_{TR}(t) \end{aligned} \quad (26)$$

where $C_P(t)$ is the price of the primary energy, $C_E(t)$ is the electricity price, and $C_T(t)$ is the price of tertiary commodity/product.

2.4 Problem Formulation

With all of the problem elements defined, the economic feasibility of a candidate IES can be assessed through the optimization of

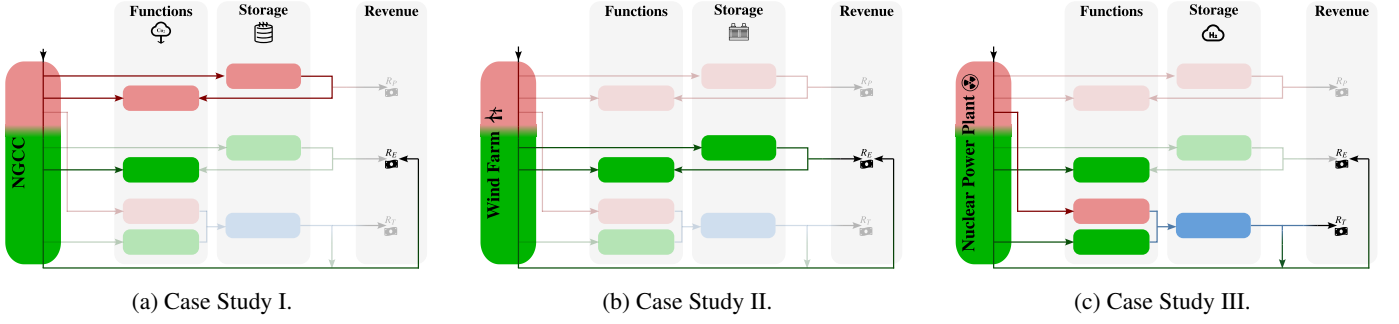


FIGURE 2: IES candidate for Case Study I: A natural gas combined cycle power plant with thermal storage and a carbon capture and storage system, Case Study II: A wind farm with a battery energy storage system, and Case Study III: A nuclear power plant with a hydrogen production (through high-temperature steam electrolysis) and storage facility.

capacity and dispatch within an all-at-one problem formulation:

$$\begin{aligned} \text{maximize:} \quad & \text{NPV}(t, \mathbf{u}, \mathbf{x}, \Sigma, \mathbf{d}) \\ & \mathbf{u}(t), \mathbf{x}(t), \Sigma \end{aligned} \quad (27a)$$

$$\text{subject to:} \quad \mathbf{g}(t, \mathbf{u}, \mathbf{x}, \mathbf{p}, \mathbf{d}) \leq \mathbf{0} \quad (27b)$$

$$\dot{\mathbf{x}} - \mathbf{f}(t, \mathbf{u}, \mathbf{x}, \mathbf{p}, \mathbf{x}_0, \mathbf{d}) = \mathbf{0} \quad (27c)$$

$$\mathbf{x}(t_0) = \mathbf{x}_0 \quad (27d)$$

$$\mathbf{x}(t_f) = \mathbf{x}(t_0) \text{ (optional)} \quad (27e)$$

$$\text{where:} \quad \mathbf{u} = \mathbf{u}(t), \mathbf{x} = \mathbf{x}(t) \quad (27f)$$

$$t \in [t_0, t_f], t_f = Nt_p \quad (27g)$$

where \mathbf{d} is the vector of problem parameters, $\mathbf{g}(\cdot)$ is the vector of inequality constraints, associated with Eqs. (9)–(15c) and Eq. (27c) refers to systems dynamics described in Eqs. (5) and (6). Periodic conditions are defined in Eq. (27g) using a base period t_p , and the number of repetitions, N . Periodic conditions can be adjusted by the user based on the availability of price signals, time horizon of the problem of interest, and other factors. For further clarification, this formulation is accompanied by Tab. 5, which provides a lexical interpretation for some of problem elements. In addition, an optimization model graph, presented in Fig. 10, is created in Sec. 5 to better assess the relationship between various problem elements.

As it is well established in mathematical optimization literature, the choice of units can negatively affect the problem's scaling and decrease its effectiveness [20]. Artfully changing the order of magnitude of problem elements can result in a more computationally-favorable problem, preventing unstable and inefficient algorithmic calculations [21]. As an example, solving the case studies in this article without appropriate scaling using 10^{-6} solver tolerance can take up as much as a day of computational time. This is because the optimizer will spend a tremendous amount of time optimizing for 10^{-6} th of a dollar value. From a broader perspective, it is clear that 10^{-6} th of a dollar value is insignificant over the project's lifetime, which has an NPV value in the order of millions of dollars. Using a scaling factor of 10^9 for the objective function and appropriately-

selected scaling factors for other problem elements, the problem can be solved in less than 300 seconds, signifying a dramatic increase in computational efficiency. Using the same solver tolerance of 10^{-6} , the objective function will be optimal up to 99.9999% of the NPV value. A more comprehensive discussion on scaling in dynamic optimization problems is discussed in Ref. [21].

3 Case Studies

This section shows several case studies to demonstrate the capabilities of the proposed framework. These studies are selected to highlight, to the extent possible, different modes of operation using different technologies and storage types. Shared parameters among these technologies are described in Table 1.

ECOGEN-CCD uses an hourly time mesh within DTQP by default, although other time intervals (e.g., decisions being made every minute) can be used as desired. The control decisions over these intervals are piecewise constant, making the zero-order hold method suitable as it produces no discretization error for the state dynamics. The resulting capacity and dispatch optimization problem, with the current assumptions outlined in the previous section, is a linear optimization problem. Due to the problem's convexity property, it can efficiently solved for the global optimal solution using MATLAB's linprog optimization solver (although other solvers could be used given the problem matrices from DTQP). A solver tolerance of 10^{-6} was used in quadprog, with an interior-point-convex algorithm to solve a dynamic optimization problem using direct transcription with an equidistant mesh and a composite Euler forward quadrature method.

Problem setup and solving times presented are associated with a single desktop workstation with an AMD Ryzen 9 3900X 12-core processor at 3.79 GHz, 32 GB of RAM, 64-bit windows 10 Enterprise LTSC version 1809, and Mat1ab R2024a.

TABLE 1: Cost parameters for generator and storage technologies used in Case Study I, II, and III.

Parameters	Generator				Storage				
	CC [22]	Wind [22]	Nuclear [22]	Unit	TES [9]	BESS [22]	Unit	Hydrogen [23]	Unit
Nom. cap.	1083	200	2156	MW	-	50	MW	640	tpd
C_{occ}	958000	1265000	6041000	\$/MW	1048947	347000	\$/MWh	600.074	\$/kg
C_{fom}	12200	26340	121640	\$/MW-yr	4.7897	0.7178	\$/MWh-h	0	\$/kg-yr
C_{vom}	1.87	0	2.37	\$/MWh	0.75	0	\$/MWh	0.2884	\$/kg

3.1 Case Study I: Combined Cycle with Thermal Storage and Carbon Capture

To meet potential environmental requirements, fossil fuel-based generators, such as NGCC power plants, are considering a reduction in their carbon emissions through CCS functions. However, inclusion of a CCS reduces the net plant efficiency and power output, while increasing the cost of electricity [24]. A potential mitigating solution is to integrate the system with a thermal energy storage (TES), as discussed in detail in Refs. [9, 25].

This study assumes that the NGCC power plant is accompanied by a CCS unit that operates only when the plant is running. The CCS function is characterized by a thermal and electrical load, which are required for the operation of CCS unit and are defined as a fixed percentage of the generator's power level. Therefore, whenever the generator is on, these electrical and thermal loads appear in the problem and must be satisfied. Including a hot thermal storage unit in the architecture enables operators to practically remove some of the parasitic thermal load from the power plant when the electricity prices are high, resulting in maximizing revenue. The considered system is illustrated in Fig. 2a, and specific, technology-dependent parameters are shown in Tab. 2.

TABLE 2: Parameters associated with Case Study I for combined cycle generator with CCS, and a thermal storage system largely based on Ref. [9].

Field	Value	Unit	Field	Value	Unit
ρ_{fuel}	146.952	kg/h.MW	α_{CO_2}	0.0029	ton/kg
τ	0.1389	h	η_G	1	-
$u_{G,min}$	0	MW	$u_{G,max}$	1083	MW
$x_{G,min}$	0	MW	$x_{G,max}$	1083	MW
$x_S(t_0)$	25	MWh	$x_G(t_f)$	25	MWh
\vec{u}_{max}	200	MW	\vec{u}_{max}	200	MW
L_P	$0.1x_G$	MW	L_E	$0.2x_G$	MW
T_{con}	3	years	r	0.075	-

The problem is carried out for 30 years of operation with an hourly time mesh (262980 time grid points), and it is assumed

that thermal energy can not be directly sold, rather, it can only be used for meeting the thermal load demand from CCS. The input parameters associated with this case study, which are largely based on Refs. [9]–[22] and are tabulated in Tables 1 and 2. Due to linearity and convexity, a global optimal solution is found, efficiently, in only 280 [s]. The results from this case study are discussed in the following and shown in Figs. 3 and 4.

The behavior of the candidate generator and storage system within the optimization problem is tightly associated with the cost of fuel and electricity. This study assumes that fuel prices are constant within each month. To understand the impact of electricity price signal on the system's behaviors, we first interpret the results within a single month, with fixed fuel prices. We have marked Fig. 3, with time periods ① and ②, which are associated with low and high electricity prices, respectively.

Accordingly, as shown in Fig. 3a, in the region marked by ①, electricity prices are low. Thus, operating the generator at full capacity is not profitable. However, this time window is a good opportunity for the generator to charge the storage, as shown in Fig. 3b. Figure 3c shows the charge and discharge signals during this period. Note that while both charging and discharging signals are active, the charging signal is larger, resulting in an increase in the storage state. During this period, the power sold to the grid is relatively lower than other time periods, as shown in Fig. 3d.

The region marked by ② describes the system's response to a scenario in which the electricity prices are relatively high. During this period, it is profitable for the generator to run at full or high capacity (see Fig. 3a). According to Figs. 3b and 3c, high electricity prices also incentivize storage discharge during this period. The discharged thermal energy during this phase removes the dependent thermal load from the generator, allowing an increase in the amount of electricity sold to the grid. This is shown in Fig. 3d.

To understand how the system behavior is affected by the combination of electricity and fuel prices, a longer horizon, during which, both price signals change, is presented in Fig. 4. From this figure, it is clear that when the electricity prices are low, and the fuel prices are high, the operation of the generator drops significantly to about 10% of its nominal capacity. This figure provides insights on the impact of fuel and electricity prices on

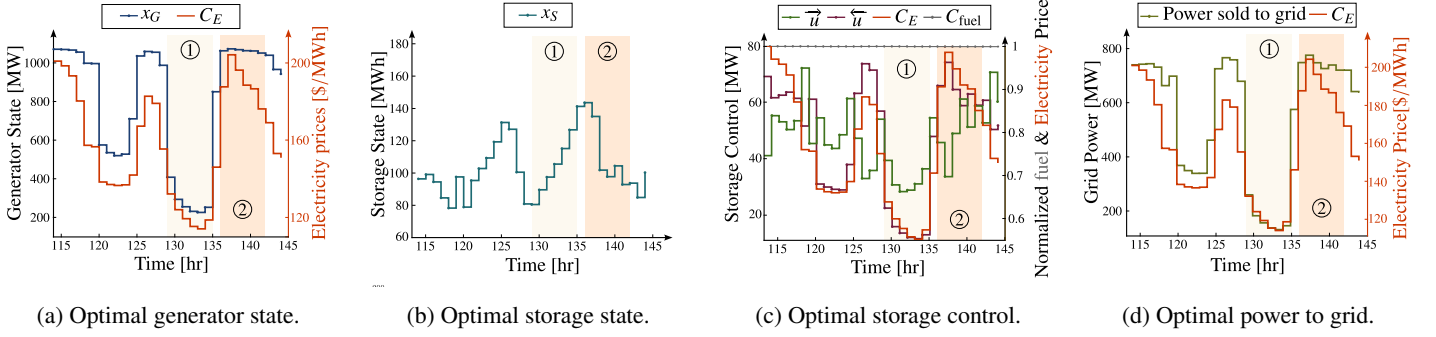


FIGURE 3: Case Study I: Optimal state and control variables for combined cycle generator with thermal storage and carbon capture.

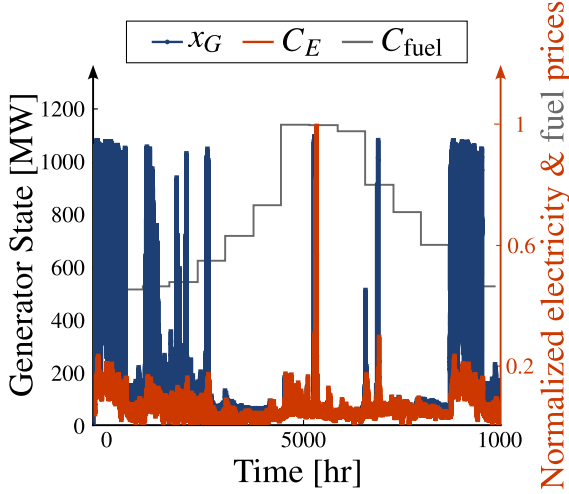


FIGURE 4: Case Study I: Optimal generator state with electricity and fuel prices over a long horizon.

system's behaviour, incentivizing the inclusion of future price increase (due to inflation, etc.) in our future work.

Overall, the optimal storage capacity is found to be 237.53 MWh, and the NPV objective is $\$ -2.99 \times 10^9$. These results are using several critical assumptions that should be reconsidered for evaluating a specific site location. Furthermore, current historical market signals were extrapolated from [26, 27], but including predicted future market signals (e.g., from Ref. [14, 28]) could aid in the decision making by considering the future grid composition and climate change. Even with these current assumptions, the expected trends are observed, and ECOGEN-CCD can be used as a strong framework for early-stage investigation of these generator and storage technologies.

Insights regarding the optimal operation of the plant can be obtained by assessing the share of various functions, and requirements over the lifetime of the plant. Specifically, Fig. 5 shows how the energy produced by the generator is utilized. Specifi-

cally, 70% of the generator energy is sold to the electricity grid, while 20%, 6.39%, and 3.61% is used for electric load, charge, and primary load, respectively. The relatively small share of the generator in satisfying the primary load is made possible through the inclusion of the thermal energy system, which, according to Fig. 5b, is responsible for satisfying 63.9% of the thermal energy demand from CCS. As shown in Fig. 5c, the storage system is responsible for about 9.09% of the overall revenue.

3.2 Case Study II: Wind Farm with Battery Energy Storage Units

In this case study, we consider an on-shore wind farm with a large plant footprint operating at 200 [MW] in the Great Plains region in combination with a 50 [MW] battery storage rate. The wind farm parameters are based on a case with 71 wind turbines, and a nominal capacity of $p_{\text{rated}} = 2.8$ [MW], with a rotor diameter of $D = 125$ [m] and a hub height of 90 [m] [22]. The battery system considered here is a utility-scale lithium-ion battery, consisting of 25 modular, prefabricated battery storage container buildings [22]. Further details about the parameters used here can be found in Ref. [22].

As opposed to Case Study I, where the operator can request a specific power output from the generator, the wind farm operation is primarily determined by the availability of wind. Using wind speed $v_w(t)$ as an additional time-dependent input to the model, the upper bound of Eq. (11) was estimated for each turbine based on the wind speeds, wind farm specifications, and the capacity factor of $c_p = 0.55$:

$$p_w = c_p \frac{1}{2} \rho_{\text{air}} \frac{\pi D^2}{4} v_w(t)^3 \quad (28)$$

where p_w is the wind power, and ρ_{air} is the air density. The maximum wind power is assumed to happen at $v_w = 25$ [m/s], and the turbine is off for wind speeds above this value. All of the power vector elements greater than p_{rated} are saturated at this value. Finally, the available power output takes into consideration the number of wind turbines in the farm. The input parameters associated with this case study are tabulated in Tables 1 and 3. The

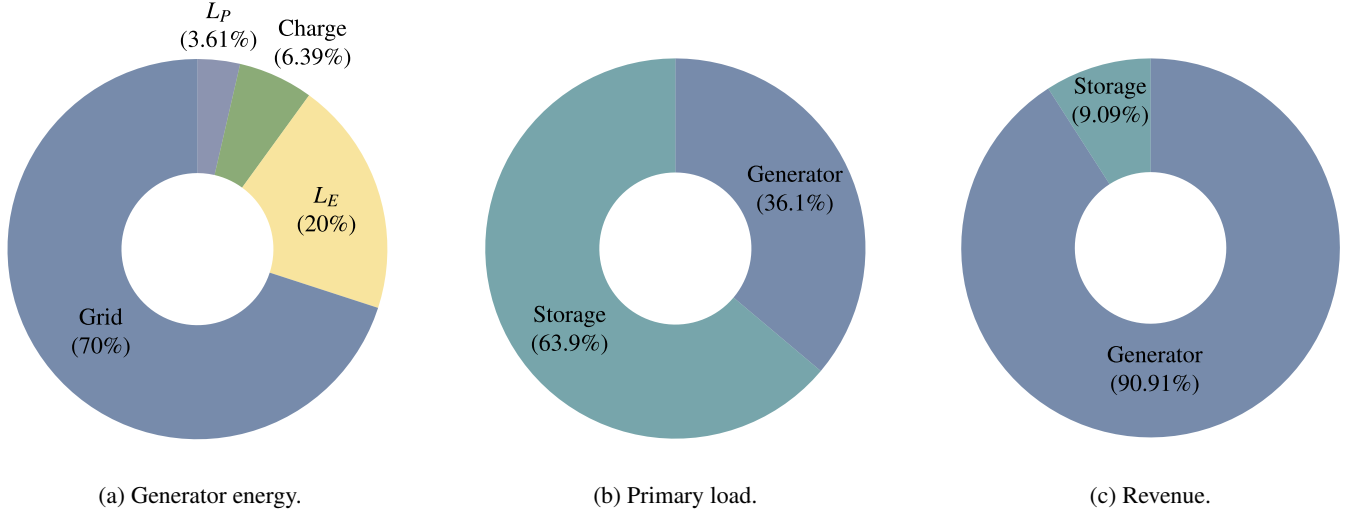


FIGURE 5: Breakdown of various elements in Case Study I, a combined cycle with thermal storage and carbon capture: (a) Generator energy usage, (b) Primary load contributions, and (c) Revenue contributions.

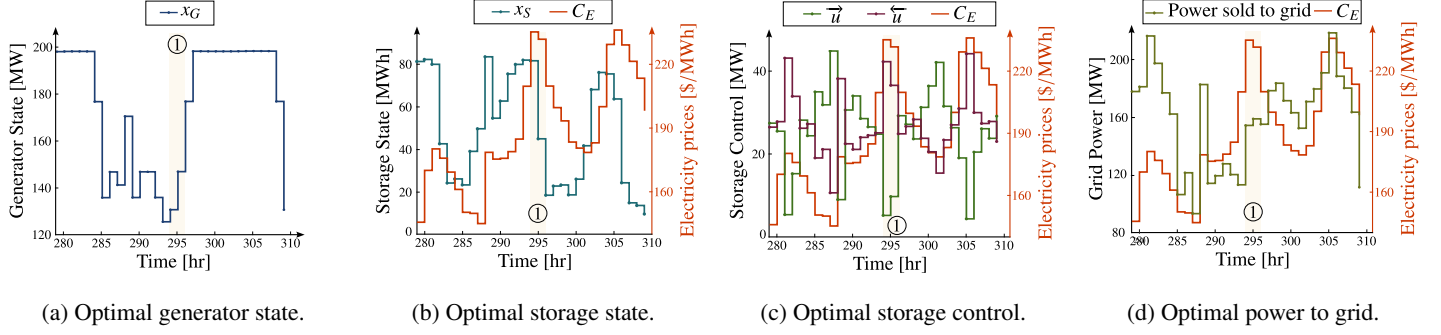


FIGURE 6: Case Study II: Optimal state and control variables for a wind farm with a battery storage unit.

candidate system is illustrated in Fig. 2b, where the electrical load is present due to the need to operate auxiliary equipment in the facility (auxiliary loads).

Unlike the previous case, here, the generator power level is mainly determined by the availability of wind, and wind turbine characteristics. Therefore, in Fig. 6a, the generator captures all the wind power that it is capable of harvesting. On the other hand, the charge and discharge decisions are heavily determined by the electricity prices. As it is clear from Fig. 6c, when the electricity prices are high, the charge signal decreases, and the discharge signal increases. This results in dramatic drops in the storage state, as evidenced by region ①, in Figs. 6b and 6c. Ideally, this outcome should result in an increase in the power sold to the grid, and thus, increased revenue. However, since the wind power available in this period is relatively lower than the neighboring time periods (see Fig. 6a), the power sold to the grid remains comparatively low. This is shown in Fig. 6d.

TABLE 3: Parameters associated with Case Study II for a wind farm connected to a battery energy storage system, largely based on Ref. [22].

Field	Value	Unit	Field	Value	Unit
ρ_{fuel}	0	kg/h.MW	α_{CO_2}	0	ton/kg
τ	0	h	η_G	1	-
$u_{G,\min}$	0	MW	$u_{G,\max}$	200	MW
$x_{G,\min}$	0	MW	$x_{G,\max}$	200	MW
$x_S(t_0)$	15	MWh	$x_G(t_f)$	15	MWh
\vec{u}_{\max}	50	MW	\vec{u}_{\max}	50	MW
L_P	0	MW	L_E	$0.1x_G$	MW
T_{con}	5	years	r	0.075	-

The optimal storage capacity is 92.45 [MWh], and the NPV

objective function is $\$ 0.69 \times 10^9$, indicating that for a large wind farm, a utility-scale BESS has the potential to be economically competitive. The percentages associated with the energy produced by the generator, and the shares of the generator and storage unit from the electrical load and revenue are shown in Fig. 7. Accordingly, it is evident that 15.2% of the generated energy is used for charging the BESS, while 5.25% is used to satisfy the electric load demands. Over the life of the project, 47.5% of this load demand is satisfied by the storage and the remainder is satisfied by the generator. Finally, storage contributions to the revenue is estimated as 17.5%.

3.3 Nuclear Power Plant with Hydrogen Generation

Nuclear power plants (NPPs) play a crucial role in the future of the electricity market, as after hydro power, they are the largest energy source with low carbon emissions [29]. Nevertheless, their economic viability is challenged by low electricity prices from other generation sources, as well as complexities of the electricity grid. On the other hand, hydrogen market has witnessed a tremendous growth in the U.S. and globally, increasing more than threefold since 1975 [30]. The growing market for hydrogen signifies a unique opportunity for NPPs to expand into additional markets, since the integration of NPPs with additional markets and technologies has the potential to keep NPPs competitive [3, 23, 31].

This case study considers the integration of NPP with a hydrogen facility and storage. This hybrid operation [23] releases NPPs from their traditional baseload by enabling them to strategically (based on economics) produce hydrogen or sell electricity to the grid. Here, we consider an NPP with two pressurized water reactors (PWR), in which, the heat generated by the fuel in the reactor is released into the surrounding pressurized cooling water. The pressurized water absorbs the heat without boiling, and after passing through a steam generator, flows through a steam turbine to generate electricity. Hydrogen is produced via high-temperature steam electrolysis (HTSE) process [32], which requires both thermal and electrical connections to NPP. Based on load requirements reported in Ref. [23], this study assumes that for every unit of electricity, 10% thermal energy is required to produce hydrogen. The thermal requirement is then defined as a function of the input electricity from the tertiary charging signal, effectively ensuring that the thermal loads are only present when a decision to produce hydrogen is made. The cost of the fuel is constructed based on predictions presented in Ref. [33], while hydrogen market prices are assumed to be fixed at \$7.0 per kg of hydrogen, which is within the price range reported in Ref. [34]. The cost parameters for the NPP and the hydrogen generation and storage facility, which are largely based on Refs. [22, 23], are described in Tab. 1. The remaining problem parameters are shown in Tab. 4.

Informed by hydrogen market operations, and the fact that sales of hydrogen can only occur at pre-scheduled times, this case

study considers a discrete daily demand through the following constraint:

$$0 \leq u_{TR}(t) \leq \begin{cases} u_{\max}, & \text{if } t = 8 \text{ AM} \\ 0, & \text{otherwise} \end{cases} \quad (29)$$

According to this equation, hydrogen sales can only occur between 8 – 9 AM on a daily basis.

TABLE 4: Parameters associated with Case Study III for a nuclear power plant connected to a hydrogen production and storage facility, largely based on Refs.[22, 23, 31, 35, 36].

Field	Value	Unit	Field	Value	Unit
ρ_{fuel}	0.001	kg/h.MW	α_{CO_2}	0	ton/kg
τ	1.79	s	η_G	1	-
$u_{G,\min}$	0	MW	$u_{G,\max}$	2156	MW
$x_{G,\min}$	0	MW	$x_{G,\max}$	2156	MW
$x_S(t_0)$	500	kg	$x_G(t_f)$	500	kg
\vec{u}_{\max}	1065	MW	\vec{u}_{\max}	27990	kg/h
L_P	$0.1\vec{u}$	MW	L_E	$0.1x_G$	MW
T_{con}	7	years	r	0.075	-
α_{ET}	0.0377	MWh/kg	α_{TE}	29.762	kg/MWh

The problem is solved for 30 years of operation, and the results are presented in Fig. 8. According to Fig. 8a, the NPP power level drops significantly in region ①, where the electricity prices are low and increases in region ② where electricity prices are high. As evidenced by Fig. 8b, during phase ① and ②, the level of hydrogen storage increases, and decreases, respectively. According to Fig. 8c, direct sales of hydrogen, which become possible everyday between 8 – 9 AM, results in a periodic discharge of hydrogen, in which the majority of the discharged hydrogen is directly sold to the market. The power sold to the grid is shown in Fig. 8d, where it is evident that the power sold to the grid is high in region ②, when the electricity prices are high.

The optimal storage capacity is 15079 [kg], with the NPV objective function of $\$ -7.92 \times 10^9$, indicating that under current assumptions, including retail prices, facility costs, and lifetime of the farm, the project needs further time to become profitable. Figure 9a indicates that from the total generator's energy, 72.04% was directly sold to the electricity grid, while 16% was used for charging the tertiary hydrogen storage, 10% used to satisfy auxiliary electrical loads, and 1.6% used to satisfy the primary load demand for HTSE. In this case study and with the presented assumptions, the storage is responsible for 7.29% of the generated revenue over the lifetime of the project. This is shown in Fig. 9b.

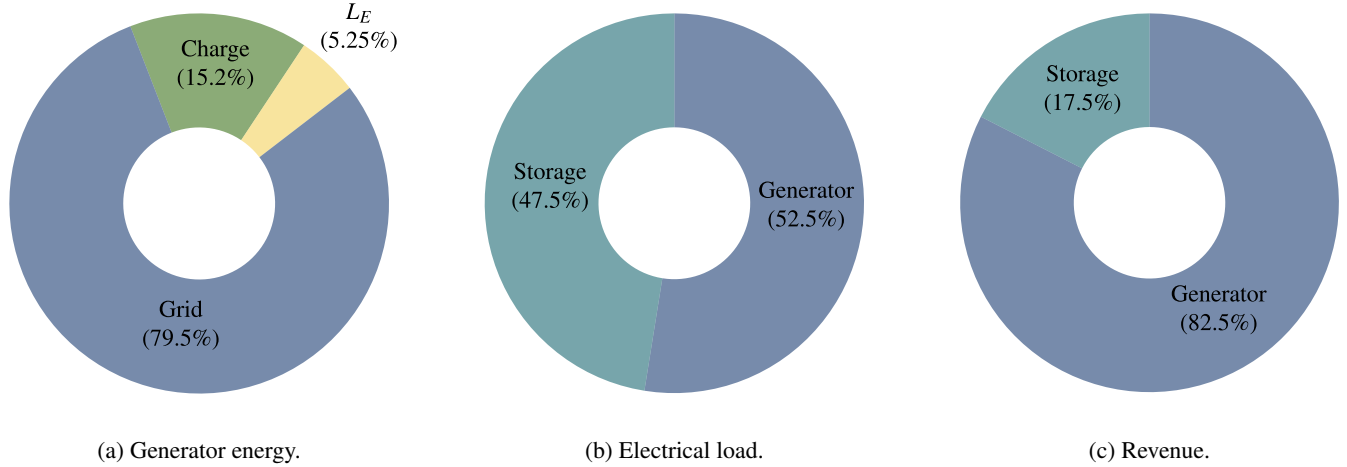


FIGURE 7: Breakdown of various elements in Case Study II, a wind farm with battery energy storage units: (a) Generator energy usage, (b) electrical load contributions, and (c) Revenue contributions.

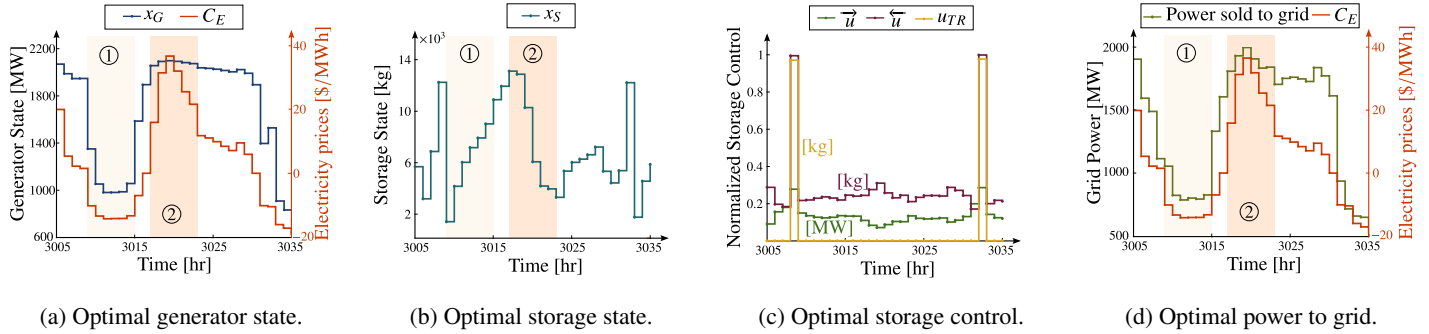


FIGURE 8: Case Study III: Optimal state and control variables for a nuclear power plant with a hydrogen production and storage facility.

4 CONCLUSION

In this article, we developed an efficient framework to assess the economic feasibility of integrated generator and storage energy systems. The proposed framework, referred to as ECOGEN-CCD, empowers the early-stage investigations of various concepts and configurations of integrated energy systems. It leverages a system-level, control co-design approach to identify the most profitable technology parameters and operations under specific assumptions. ECOGEN-CCD has the potential to offer unique insights for both new projects and retrofit efforts, facilitating the decision making process and communications among technology experts, investors, and stakeholders.

The capabilities of ECOGEN-CCD were tested for three case studies. Case Study I was focused on a power plant that includes a natural gas combined cycle generator, a thermal storage unit, and a carbon capture and storage system. Case Study II considered a wind farm with a battery storage system, thereby bring-

ing up some of the complexities in dealing with non-dispatchable renewable technologies. Hybrid operation of a nuclear power plant with a hydrogen generation and storage facility was assessed in Case Study III. Since in its current form, ECOGEN-CCD solves a linear, convex optimization problem, the case studies were investigated for the duration of 30 years, on an hourly basis, in an efficient manner identifying the global optimal solution.

As a next step, it is desirable to enable the framework to account for the simultaneous presence of multiple storage types and other heterogeneous and more complex configurations. This framework, within its current and future capabilities, has the potential to further improve the economic viability of various integrated energy systems and decision-making surrounding them.

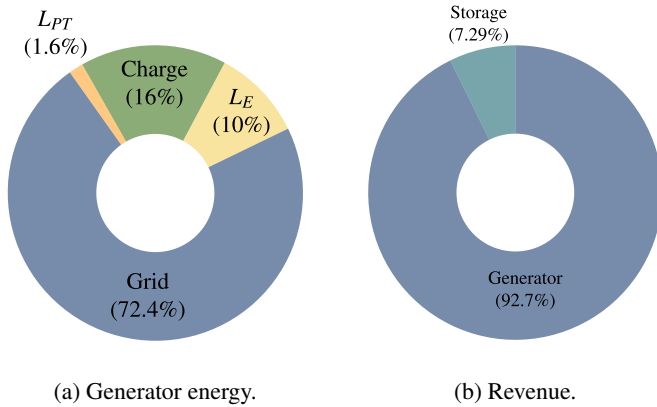


FIGURE 9: Breakdown of various elements in Case Study III, a nuclear power plant with hydrogen generation and storage facility: (a) Generator energy usage, (b) Revenue contributions.

ACKNOWLEDGMENT

The authors would like to thank Ian Goven and Roberto Vercellino for their contributions to the development of this research.

REFERENCES

- [1] Wu, J., Yan, J., Jia, H., Hatziaargyriou, N., Djilali, N., and Sun, H., 2016. "Integrated energy systems". *Appl. Energy*, **167**, Apr., pp. 155–157. doi: [10.1016/j.apenergy.2016.02.075](https://doi.org/10.1016/j.apenergy.2016.02.075)
- [2] Berjawi, A., Walker, S., Patsios, C., and Hosseini, S., 2021. "An evaluation framework for future integrated energy systems: A whole energy systems approach". *Renew. Sustain. Energy Rev.*, **145**, July, p. 111163. doi: [10.1016/j.rser.2021.111163](https://doi.org/10.1016/j.rser.2021.111163)
- [3] Zhang, T., 2022. "Techno-economic analysis of a nuclear-wind hybrid system with hydrogen storage". *J. Energy Storage*, **46**, Feb., p. 103807. doi: [10.1016/j.est.2021.103807](https://doi.org/10.1016/j.est.2021.103807)
- [4] Arent, D. J., Bragg-Sitton, S. M., Miller, D. C., Tarka, T. J., Engel-Cox, J. A., Boardman, R. D., Balash, P. C., Ruth, M. F., Cox, J., and Garfield, D. J., 2021. "Multi-input, multi-output hybrid energy systems". *Joule*, **5**(1), Jan., pp. 47–58. doi: [10.1016/j.joule.2020.11.004](https://doi.org/10.1016/j.joule.2020.11.004)
- [5] HERON: Overview, a broad look at the holistic energy resource optimization network software. <https://ies.inl.gov/Training%20Documents/Day%201%2003-%20HERON%20Overview.pdf>
- [6] McDowell, D., Talbot, P., Wrobel, A., Frick, K., Bryan, H., Boyer, C., Boardman, R., Taber, J., and Hansen, J., 2021. A techno-economic assessment of LWR flexible operation. Tech. rep., Dec. doi: [10.2172/1844211](https://doi.org/10.2172/1844211)
- [7] Khamis, I., and Malshe, U., 2010. "HEEP: A new tool for the economic evaluation of hydrogen economy". *Int. J. Hydrog. Energy*, **35**(16), Aug., pp. 8398–8406. doi: [10.1016/j.ijhydene.2010.04.154](https://doi.org/10.1016/j.ijhydene.2010.04.154)
- [8] Garcia-Sanz, M., 2019. "Control co-design: An engineering game changer". *Adv. Control Appl.*, **1**(1), Oct. doi: [10.1002/adc2.18](https://doi.org/10.1002/adc2.18)
- [9] Vercellino, R., Markey, E., Limb, B. J., Pisciotta, M., Huyett, J., Garland, S., Bandhauer, T., Quinn, J. C., Psarras, P., and Herber, D. R., 2022. "Control co-design optimization of natural gas power plants with carbon capture and thermal storage". In Volume 3A: 48th Design Automation Conference (DAC), IDETC-CIE2022, American Society of Mechanical Engineers. doi: [10.1115/detc2022-90021](https://doi.org/10.1115/detc2022-90021)
- [10] Soto Gonzalez, G., and Talbot, P., 2022. Force-dispatches integration - initial demonstration. Tech. rep., Sept. doi: [10.2172/1891636](https://doi.org/10.2172/1891636)
- [11] Li, B., Talbot, P., McDowell, D., and Hansen, J., 2021. Release a public version of HERON (HERON 2.0) with improved algorithms for the treatment of energy storage. Tech. rep., Dec. doi: [10.2172/1838610](https://doi.org/10.2172/1838610)
- [12] Herber, D. R., 2017. "Advances in combined architecture, plant, and control design". Ph.D. Dissertation, University of Illinois at Urbana-Champaign, Urbana, IL, USA, Dec.
- [13] Herber, D. R., Lee, Y., and Allison, J. DT QP project. <https://github.com/danielrherber/dt-qp-project>
- [14] MIT Energy Initiative and Princeton University ZERO lab. GenX. <https://github.com/GenXProject/GenX>
- [15] <https://github.com/AzadSaeed/ECOGEN-CCD> (will be updated in the final submission).
- [16] Joskow, P. L., and Parsons, J. E., 2009. "The economic future of nuclear power". *Daedalus*, **138**(4), Sept., pp. 45–59. doi: [10.1162/daed.2009.138.4.45](https://doi.org/10.1162/daed.2009.138.4.45)
- [17] Mantripragada, H., and Rubin, E., 2018. "Techno-economic analysis methods for nuclear power plants". *SSRN*. doi: [10.2139/ssrn.3198421](https://doi.org/10.2139/ssrn.3198421)
- [18] IAEA, 2013. Approaches for assessing the economic competitiveness of small and medium sized reactors. Tech. Rep. NP-T-3.7, Vienna.
- [19] Wealer, B., Bauer, S., Hirschhausen, C., Kemfert, C., and Göke, L., 2021. "Investing into third generation nuclear power plants". p. 110836. doi: [10.1016/j.rser.2021.110836](https://doi.org/10.1016/j.rser.2021.110836)
- [20] Martins, J. R. R. A., and Ning, A., 2021. *Engineering Design Optimization*. Cambridge University Press, Nov. doi: [10.1017/9781108980647](https://doi.org/10.1017/9781108980647)
- [21] Herber, D. R., and Allison, J. T., 2017. "Unified scaling of dynamic optimization design formulations". In Volume 2A: 43rd Design Automation Conference, IDETC-CIE2017, American Society of Mechanical Engineers.
- [22] Administration, E. I., 2020. Capital cost and performance characteristic estimates for utility scale electric power generating technologies. Tech. rep.
- [23] Frick, K., Talbot, P., Wendt, D., Boardman, R., Rabiti, C., Bragg-Sitton, S., Ruth, M., Levie, D., Frew, B., Elgowainy, A., and Hawkins, T., 2019. Evaluation of hydrogen production feasibility for a light water reactor in the Midwest. Tech. rep., Sept. doi: [10.2172/1569271](https://doi.org/10.2172/1569271)
- [24] Rubin, E. S., and Zhai, H., 2012. "The cost of carbon capture and storage for natural gas combined cycle power plants". *Environ. Sci. Technol.*, **46**(6), Mar., pp. 3076–3084. doi: [10.1021/es204514f](https://doi.org/10.1021/es204514f)
- [25] Limb, B. J., Markey, E., Vercellino, R., Garland, S., Pisciotta, M., Psarras, P., Herber, D. R., Bandhauer, T., and Quinn, J. C., 2022. "Economic viability of using thermal energy storage for flexible carbon capture on natural gas power plants". *J. Energy Storage*, **55**, Nov., p. 105836. doi: [10.1016/j.est.2022.105836](https://doi.org/10.1016/j.est.2022.105836)
- [26] Grid status. <https://docs.gridstatus.io/en/latest/search.html?q=cite#>
- [27] <https://www.eia.gov/dnav/ng/hist/rngwhhdm.htm>
- [28] Jenkins, J. D., Chakrabarti, S., Cheng, F., and Neha, P., 2021. Summary report of the GenX and PowerGenome runs for generating price series (for ARPA-E FLECCS Project). doi: [10.5281/ZENODO.5765798](https://doi.org/10.5281/ZENODO.5765798)
- [29] BP statistical review of world energy. <http://large.stanford.edu/courses/2016/ph240/stanchi2/docs/bp-2016.pdf>
- [30] The future of hydrogen: Seizing today's opportunities. <https://www.iea.org/reports/the-future-of-hydrogen>
- [31] Hancock, S., and Westover, T., 2022. "Simulation of 15% and 50% thermal power dispatch to an industrial facility using a flexible generic full-scope pressurized water reactor plant simulator". *Energies*, **15**(3), Feb., p. 1151. doi: [10.3390/en15031151](https://doi.org/10.3390/en15031151)
- [32] Mingyi, L., Bo, Y., Jingming, X., and Jing, C., 2008. "Thermodynamic analysis of the efficiency of high-temperature steam electrol-

- ysis system for hydrogen production”. *J. Power Sources*, **177**(2), Mar., pp. 493–499. 10.1016/j.jpowsour.2007.11.019.
- [33] Kryzia, D., and Gawlik, L., 2016. “Forecasting the price of uranium based on the costs of uranium deposits exploitation”. *Mineral Resources Management*, **32**(3), Sept., pp. 93–110. doi: [10.1515/gospo-2016-0026](https://doi.org/10.1515/gospo-2016-0026)
- [34] Ramadan, M. M., Wang, Y., and Tooteja, P., 2022. “Analysis of hydrogen production costs across the united states and over the next 30 years”. doi: [10.48550/arXiv.2206.10689](https://doi.org/10.48550/arXiv.2206.10689)
- [35] Settle, F. A., 2009. “Uranium to electricity: The chemistry of the nuclear fuel cycle”. *J. of Chem. Educ.*, **86**(3), Mar., p. 316. doi: [10.1021/ed086p316](https://doi.org/10.1021/ed086p316)
- [36] OECD and Nuclear Energy Agency, 2021. Technical and economic aspects of load following with nuclear power plants. Tech. rep. doi: [10.1787/29e7df00-en](https://doi.org/10.1787/29e7df00-en)

5 APPENDIX

This section includes some complementary information, providing more details for improved understanding of the paper.

A Node Definitions

Mathematical description of the nodes labeled in Fig. 1 are presented in this section. These equations are used to formulate inequality constraints associated with Eqs. (14)-(15), and present the available amount of power from the generator.

$$n_1 : x_G$$

$$n_2 : x_G - \vec{u}_p$$

$$n_3 : x_G - \vec{u}_p - L_{GP}$$

$$n_4 : x_G - \vec{u}_p - L_{GP} - L_{GPT}$$

$$n_5 : \eta_G(x_G - \vec{u}_p - L_{GP} - L_{GPT})$$

$$n_6 : \eta_G(x_G - \vec{u}_p - L_{GP} - L_{GPT}) - \vec{u}_E$$

$$n_7 : \eta_G(x_G - \vec{u}_p - L_{GP} - L_{GPT}) - \vec{u}_E - L_{GE}$$

$$n_8 : \eta_G(x_G - \vec{u}_p - L_{GP} - L_{GPT}) - \vec{u}_E - L_{GE} - \vec{u}_T$$

$$n_9 : \eta_G(x_G - \vec{u}_p - L_{GP} - L_{GPT}) - \vec{u}_E - L_{GE} - \vec{u}_T + \alpha_{TE} \overleftarrow{\eta}_T(\overleftarrow{u}_T - u_{TR})$$

where the power signal sent from the generator to satisfy the thermal and electrical loads are described by L_{GP} , L_{GPT} , and L_{GE} , respectively:

$$L_{GP} = L_P x_G - \overleftarrow{\eta}_P \overleftarrow{u}_p + \overleftarrow{\eta}_{PU} \overleftarrow{u}_{PR}$$

$$L_{GPT} = L_{PT} \vec{u}_T$$

$$L_{GE} = L_E x_G - \overleftarrow{\eta}_E \overleftarrow{u}_E + \overleftarrow{\eta}_{EU} \overleftarrow{u}_{ER}$$

where L_{PT} is the primary load required to operate the tertiary facilities, defined as L_T percent of the tertiary charging load. Note that these equations constitute equality constraints that are substituted within the dynamic optimization problem.

B Lexical Interpretations of Problem Elements

This section serves as a complementary section to the mathematical explanations offered throughout the article. Specifically, in

this section, we offer some lexical interpretations to facilitate the understanding of various problem elements by non-optimization experts. These interpretations are offered in Tab. 5.

Nomenclature

Acronyms

BESS	battery energy storage system
CCD	control co-design
CCS	carbon capture and storage
HES	hybrid energy systems
HTSE	high-temperature steam electrolysis
IES	integrated energy systems
NGCC	natural gas combined cycle
NPV	net present value
TES	thermal energy storage
NPP	nuclear power plant

Subscripts

\bullet_E	index for electrical domain
\bullet_G	index for generator
\bullet_P	index for primary domain
\bullet_R	index for revenue
\bullet_S	index for Storage
\bullet_T	index for tertiary domain

Select Variables

C_{cap}	capital cost
C_{fom}	fixed o&m cost
C_{vom}	variable o&m cost
E_{fuel}	fuel expenditure
R	revenue
\mathbf{u}	control vector
\mathbf{x}	state vector
Σ	storage capacity
L	Load
n	node
\vec{u}	charging signal
\overleftarrow{u}	discharging signal

TABLE 5: Lexical interpretation for select elements in the optimization problem.

Lexical interpretation	Mathematical description	Reference
The objective function is the maximization of the Net Present Value of the system over the lifetime of the power plant	maximize NPV	Eq. (16)
Generator dynamics describes the power level of the generator unit as a function of ramp rate , generator's current state , and the requested power	$\dot{x}_G(t) = \frac{1}{\tau}(-x_G(t) + u_G(t))$	Eq. (5)
Storage dynamics describes the available resource in the storage system as a function of charging , and discharging power signals, and the storage efficiencies	$\dot{x}_S(t) = \overrightarrow{\eta} \overrightarrow{u} - \overleftarrow{\eta} \overleftarrow{u}$	Eq. (6)
Storage capacity must be non-negative	$0 \leq \Sigma$	Eq. (9)
At every time instant, control variables are non-negative and upper-bounded by their maximum limit	$0 \leq u(t) \leq u_{\max}$	Eq. (10)
Revenue control signal is never greater than the control discharged power	$u_{PR}(t) \leq \overleftarrow{u}_P(t)$ $u_{ER}(t) \leq \overleftarrow{u}_E(t)$ $u_{TR}(t) \leq \overleftarrow{u}_T(t)$	Eqs. (10b)–(10d)
The generator's power level is non-negative , and upper-bounded by nominal capacity or maximum available power to harvest	$0 \leq x_G(t) \leq x_{G,\max}(t)$	Eq. (11)
The storage energy level is non-negative and never greater than storage capacity	$0 \leq x_S(t) \leq \Sigma$	Eq. (12)
The generator and storage state is prescribed at t_0 and for storage may be prescribed at t_f	$x(t_0) = x_0$ $x_S(t_f) = x_S(t_0)$	Eq. (13)
Each charging signal is upper-bounded by the available power in the generator at that node	$\overrightarrow{u}_P(t) \leq n_1(t)$ $\overrightarrow{u}_E(t) \leq n_5(t)$ $\overrightarrow{u}_T(t) \leq n_7(t)$	Eq. (14)
The generator's power signals to satisfy primary and electrical loads is non-negative and always smaller or equal to the available power in the corresponding node	$0 \leq L_{GP}(t) \leq n_2(t)$ $0 \leq L_{GPT}(t) \leq n_3(t)$ $0 \leq L_{GE}(t) \leq n_5(t)$	Eq. (15)
The available amount of power on node 1	$n_1 : x_G$	Fig. 1
The available amount of power on node 2	$n_2 : x_G - \overrightarrow{u}_P$	
The available amount of power on node 3	$n_3 : x_G - \overrightarrow{u}_P - L_{GP}$	
The available amount of power on node 4	$n_4 : x_G - \overrightarrow{u}_P - L_{GP} - L_{GPT}$	
The available amount of power on node 5	$n_5 : \eta_G(x_G - \overrightarrow{u}_P - L_{GP} - L_{GPT})$	
The available amount of power on node 6	$n_5 : \eta_G(x_G - \overrightarrow{u}_P - L_{GP} - L_{GPT}) - \overrightarrow{u}_E$	
The available amount of power on node 7	$n_6 : \eta_G(x_G - \overrightarrow{u}_P - L_{GP} - L_{GPT}) - \overrightarrow{u}_E - L_{GE}$	
The available amount of power on node 8	$n_7 : \eta_G(x_G - \overrightarrow{u}_P - L_{GP} - L_{GPT}) - \overrightarrow{u}_E - L_{GE} - \overrightarrow{u}_T$	
The available amount of power on node 9	$n_8 : \eta_G(x_G - \overrightarrow{u}_P - L_{GP} - L_{GPT}) - \overrightarrow{u}_E - L_{GE} - \overrightarrow{u}_T$ $+ \alpha_c \overleftarrow{\eta}_T \overleftarrow{u}_T - \alpha_c \overleftarrow{\eta}_T u_{TR}$	

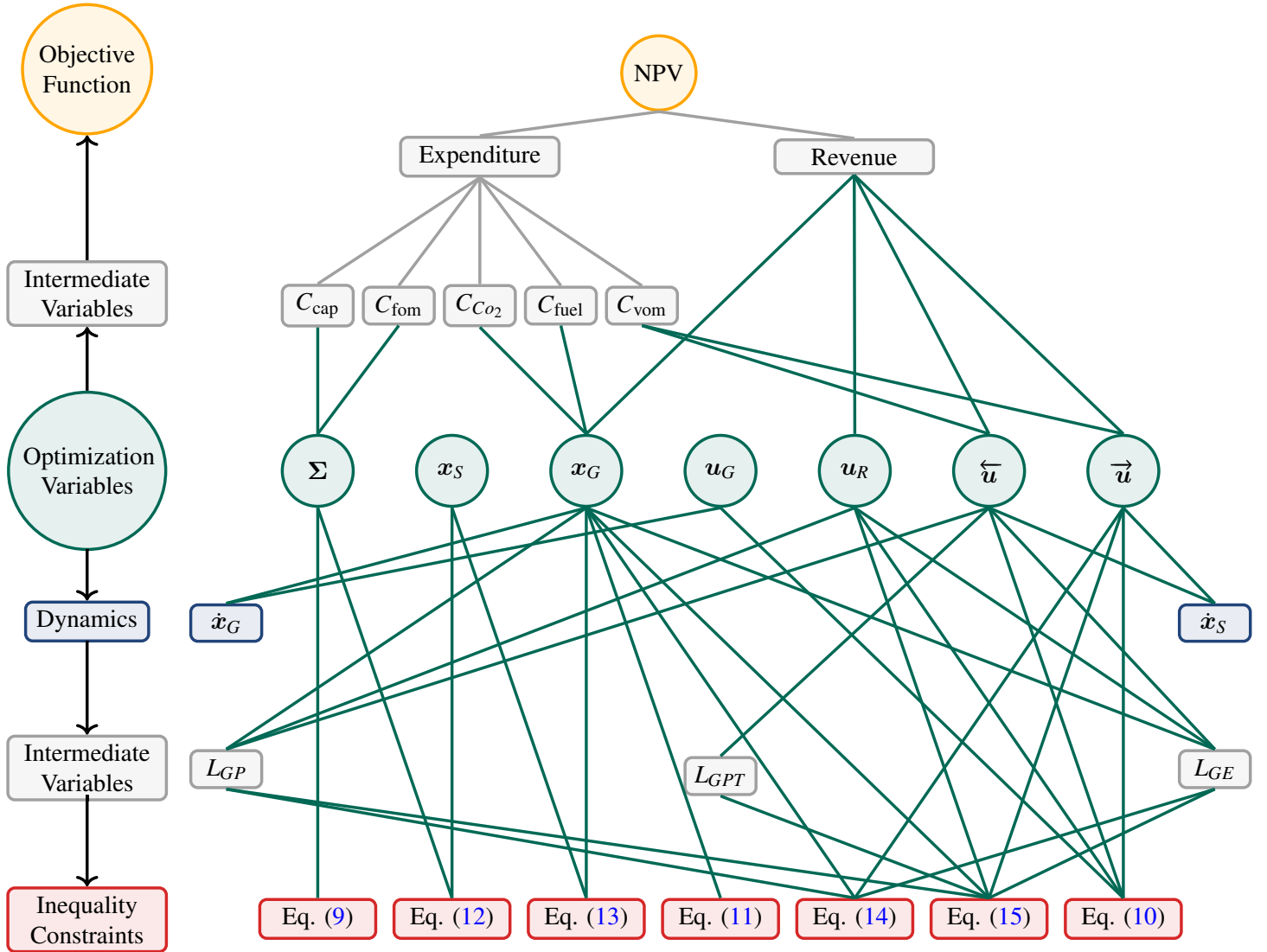


FIGURE 10: Optimization model graph for the proposed framework.